

Traffic-Tracing Gateway (TTG)

Haiping Liu, Xiaoling Qiu, Dipak Ghosal, Chen-Nee Chuah, Xin Liu, and Yueyue Fan

University of California, Davis

Email: {hpliu, xqiu, dghosal, chuah, xinliu, yyfan}@ucdavis.edu

Abstract—Traffic density in wireless networks is time- and space-varying as users move from one area to another. For example, the majority of traffic stays in residential areas in the early morning and late evening; but moves to business or commercial areas in daytime. Therefore, it is challenging to efficiently locate base stations during network planning stage, due to the time-varying traffic distribution. Base stations vary from highly congested to seldom utilized depending on time. However, measurement studies show that the movement of the traffic density is highly predictable, and the traffic always travel along similar routes among different parts in a city or town during one day or over a week. Therefore, we introduce the traffic-tracing gateway (TTG), which acts as the base station that tracks the movement of the traffic. Given the traffic distribution of a period, we design an algorithm to determine the optimal trajectories of TTGs that can cover the maximum traffic. Our solution framework can optimally deploy TTGs in the congested areas to provide better coverage and relieve congestion. Our simulation studies based on realistic user mobility show that TTGs can result in significant improvement over fixed infrastructure based network across multiple metrics in multiple scenarios.

I. INTRODUCTION

Good network planning is important to balance between two goals: 1) to provide good service to meet traffic demand; and 2) to reduce the deployment cost. However, network planning is challenging in wireless networks, due to the temporal and spatial variance of traffic demand. For instance, it was shown in [1, 2] that traffic demand changes over time primarily due to temporal variation in user mobility; the maximum demand can be more than double of the minimum at the same area.

Fortunately, detailed analysis of the traffic distribution shows that the traffic changes are not random, but have a high predictability [3]. Users and consequently the traffic generated by them usually have fixed patterns of movement during a day or a week. For example, the data from the cellular network in a city [1, 2, 4] indicate that in the early morning or at night, a large amount of traffic is generated in the residential areas; during the working hours, the majority of the traffic stay in the business or commercial areas; and in the evening, the traffic spreads in restaurants or shopping malls. Similarly, the data from the WiFi network in a university setting [5, 6] show that high workload appears in the coverage of different access points during specific time periods according to the building types (e.g., academic, residential). In the early morning or during holidays, most traffic is in the residential buildings; during the schooltime, the majority of the workloads remains in the academic buildings; and during lunch or dinner time, access points in restaurants and cafes are congested. Therefore, despite the significant traffic variance in one area, the traffic

movement patterns among multiple areas in a city or within a campus have a high degree of predictability.

Based on the observation of the stability of the traffic mobility patterns, we introduce a new component into wireless networks, called traffic-tracing gateway (TTG), which can move around in response to the change in the traffic demand. In the TTG system, the fixed network architecture provides the basic coverage and wireless resource most of the time. When a large amount of user traffic moves into a specific area, TTGs serve the additional traffic to relieve congestion. In order to efficiently re-utilize TTGs, the TTGs trace the traffic across space and time. Because traffic demand has high predictability, it is possible to derive the optimal trajectories, given the traffic distribution at different locations and at different time periods.

A base station logically has two interfaces, one connecting to the backbone network (backbone interface) and the other connecting to the customer devices (access interface). Those two interfaces typically do not interfere to avoid performance degradation. The fixed base stations often have wired connection and consequently these backbone interfaces have no interference with the wireless access interface. However, both interfaces of TTGs are wireless interfaces to support mobility, and thus need to operate on different spectrums with different technologies. Therefore, a heterogeneous wireless network is the natural choice.

Today, various wireless networks coexist, including WiFi, 2G, 3G, WiMAX and LTE networks. WiFi has become the standard wireless access technique for most laptops or smartphones, and provides the low-cost network access; the cellular access provides the constant and reliable connection; WiMAX operates on the spectrum of higher frequency, and provides larger coverage and higher throughput; and LTE Advanced is the latest mobile network technology, and is designed to provide high-speed transmissions for future applications. In the context of TTGs, the access interface usually has a small transmission range for efficient spectrum reuse and a relatively low cost. The backbone interface needs larger transmission range and higher capacity to support TTGs. Therefore, given the access interface, multiple wireless techniques can serve as the backbone interface. For example, TTGs can be equipped with WiFi or cellular as the access interface, and WiMAX or LTE Advanced with directional antennas as the backbone interface. Note that TTGs are typically more sophisticated than a typical cellular user. TTGs can have higher transmission power, larger antennas, and multiple/directional antennas. Therefore, they can utilize wireless backhaul link much more efficiently.

Figure 1 illustrates the idea of TTGs. In the figure, A , B , C ,

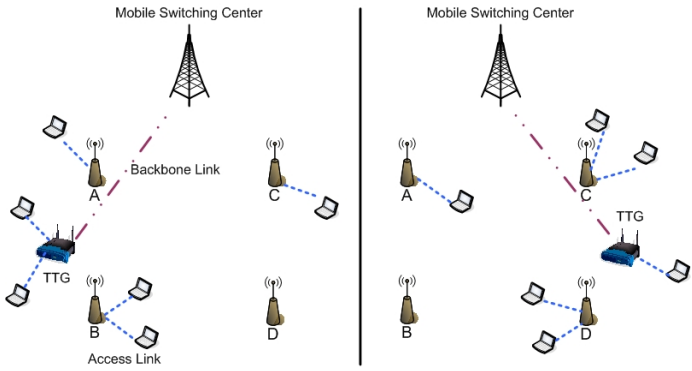


Fig. 1. Network Structure of TTG

and D are traditional base stations forming the basic network architecture with wired backhaul connections. The TTG moves along the predesigned trajectory in response to the changes in the traffic distribution and serves the congested traffic in different areas at different time, as shown in Figure 1. The TTG connects to the mobile switching center through wireless backhaul. Our goal is to find optimal trajectories for TTGs that trace the traffic. We will also address practical concerns where one cannot afford dedicated TTGs.

The rest of the paper is organized as follows. In Section II, we define the problem of finding optimal TTG trajectories, given the traffic distribution. Section III describes a dynamic programming based solution, and its practical extensions. The performance evaluation is presented in Section IV in multiple scenarios. We discuss the related work in Section V, and conclude in Section VI.

II. PROBLEM DEFINITION

The focus of this paper is to introduce a new component, TTG, to supplement the existing fixed network architecture. We focus on determining the TTG trajectories according to the traffic density distribution. In general, the TTGs are located in the areas where the traffic density is high, and move to the next position when the traffic density changes.

A. TTG Constraints

Without loss of generality, suppose the wireless network is designed to cover a rectangular area, where the location of TTG i is $[x_i(t), y_i(t)]$ at time t , and $0 \leq x_i(t) \leq X$ and $0 \leq y_i(t) \leq Y$. We consider the following two constraints:

- 1) **Speed:** The TTG is usually located on a car or a bus, which has a speed limit S . Suppose the derivative of $[x_i(t), y_i(t)]$ over t is $[\dot{x}_i(t), \dot{y}_i(t)]$. Then, without any constraint on the mobility patterns or directions,

$$\dot{x}_i(t)^2 + \dot{y}_i(t)^2 \leq S^2. \quad (1)$$

- 2) **Transmission Range:** The backbone interface of the TTG is designed to always have connection to the central base station within the area $X \times Y$. The access interface, which is designed to communicate with customer devices, usually has a transmission range constraint R , i.e., the coverage of the access interface is a circle C_i

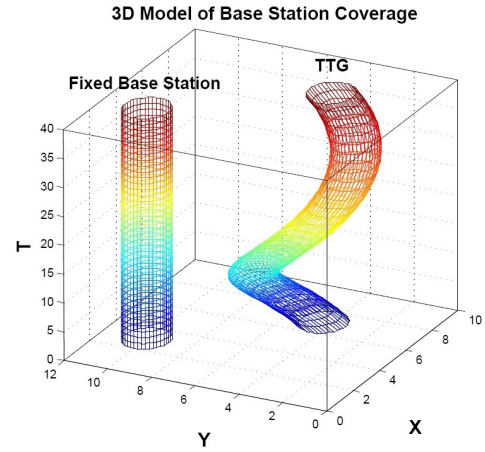


Fig. 2. 3D Model of Base Station Coverage.

with the center $[x_i(t), y_i(t)]$ and radius R . At anytime t , traffic generated at $[u, v]$ can be forwarded to TTG i iff $[u, v] \in C_i$ as

$$[u, v] \in C_i \Leftrightarrow (u - x_i(t))^2 + (v - y_i(t))^2 \leq R^2 \quad (2)$$

B. Formulation

We aim to design the optimal TTG trajectories within a given time period T , which could be a day, a week, or longer, given the traffic density function $f(u, v, t)$ that indicates the traffic density at position $[u, v]$ at time t , $0 \leq t \leq T$. Considering the time-dimension, the complete traffic distribution model becomes three dimensions $X \times Y \times T$, as shown in Figure 2 (Figure 2 is an illustration and is not scaled). In this model, the coverage of a TTG i is illustrated as $C_i([x_i(t), y_i(t)])$. For any time t , i.e., on the plane t in the 3D space, the projected area of C_i is a circle defined in Eq.(2). For a traditional fixed base station, i.e., $[x_i(t), y_i(t)] = [x_i, y_i]$, the shape of $C_i([x_i, y_i])$ is a cylinder, marked as *Fixed Base Station* in Figure 2. However, due to the movement of TTG i , $C_i([x_i(t), y_i(t)])$ becomes twisted, marked as *TTG* in Figure 2.

If we have N TTGs, the total coverage of those TTGs is the union of all C_i ,

$$\mathbb{D} = \cup_{i=1}^N C_i([x_i(t), y_i(t)]). \quad (3)$$

Therefore, designing the optimal TTG trajectories is equal to covering as much traffic as possible into \mathbb{D} .

Some wireless network measurement studies [1, 2, 5, 6] provide the traffic distribution function $f(u, v, t)$. In this model, we suppose that $f(u, v, t)$ is known as the input. Then the objective function of the optimization problem is,

$$\Omega = \max_{\mathbb{D}} \oint_{[u, v, t] \in \mathbb{D}} f(u, v, t) du dv dt, \quad (4)$$

where the optimization is taken over all possible trajectories (\mathbb{D} is the decision variable), and Eq. (1) and (2) are constraints of the objective function of Eq. (4).

TABLE I
NOTATIONS IN THE FORMULATION.

Symbol	Explanation
X, Y	Side lengths of the area
T	Time period under the analysis
S	Speed constraint of TTGs
R	Transmission range of TTGs
$[x_i(t), y_i(t)]$	Position of TTG i at time t
$[\dot{x}_i(t), \dot{y}_i(t)]$	Differential coefficient of $[x_i(t), y_i(t)]$, or the velocity vector of TTG i
C_i	Coverage of TTG i during T
$f(u, v, t)$	Traffic density distribution at point $[u, v, t]$
Ω	Maximum traffic covered by all TTGs during T
δt	Discrete temporal interval to divide T for dynamic programming, and $T = n_t \delta t$
$\delta x, \delta y$	Discrete spatial interval to divide X and Y $\delta x = \delta y = S * \delta t$
$f(k, l, h)$	Discrete format of $f(u, v, t)$ $f(k, l, h) = f(u, v, t) \delta x \delta y \delta t$
$F(\vec{x}, \vec{y}, h)$	Traffic covered by all TTGs at time h
$V(\vec{x}, \vec{y}, h)$	Maximum traffic covered by TTGs from h to n_t
$a^i(k, l, h)$	Fraction of traffic at point $[k, l, h]$ forwarded by TTG i
$V(x, y, t)$	Maximum traffic covered from t to T , from $[x, y, t]$

III. ANALYSIS AND SOLUTION

The optimization problem is complex, because in the objective function of Eq. (4): (a) $f(u, v, t)$ is not necessarily linear or convex, but can be any type of functions; and (b) \mathbb{D} is not a function of integral variables u or v , but the integral domain defined by $[x_i(t), y_i(t)]$. In order to solve this complex problem, we employ *dynamic programming*.

Dynamic programming solves a complex problem by breaking it down into simpler subproblems in a recursive manner. In this problem, we discretize the TTG trajectories across time. We divide time T into small intervals, $T = n_t \delta t$, and find the optimal locations at each time interval t that optimize the overall system performance. In order to find the solution in the discrete model, we also discretize the other two dimensions into small intervals $X = n_x \delta x$ and $Y = n_y \delta y$, and $\delta x = \delta y = S * \delta t$.

In this discrete model, we define two index variables.

- $J^i(k, l, h)$: the index variable indicating whether point $[k, l], 1 \leq k \leq n_x, 1 \leq l \leq n_y$ is in the coverage of TTG i at time $h, 1 \leq h \leq n_t$,

$$J^i(k, l, h) = \begin{cases} 1 & \text{if } [k, l, h] \in C_i \\ 0 & \text{if } [k, l, h] \notin C_i. \end{cases} \quad (5)$$

- $I(k, l, h)$: the index variable indicating whether point $[k, l], 1 \leq k \leq n_x, 1 \leq l \leq n_y$ is in the coverage of any TTG,

$$I(k, l, h) = \begin{cases} 1 & \text{if } \sum_{i=1}^N J^i(k, l, h) \geq 1 \\ 0 & \text{if } \sum_{i=1}^N J^i(k, l, h) = 0. \end{cases} \quad (6)$$

Based on the index variables, we can derive the objective function in the discrete format as:

$$\Omega = \max_{\mathbb{D}} \sum_{k=1}^{n_x} \sum_{l=1}^{n_y} \sum_{h=1}^{n_t} I(k, l, h) f(k, l, h), \quad (7)$$

where $f(k, l, h)$ is the discrete format of $f(u, v, t)$, which can be considered as

$$f(k, l, h) = f(u, v, t) \delta x \delta y \delta t, \quad (8)$$

and $(k-1)\delta x \leq u \leq k\delta x, (k-1)\delta y \leq v \leq k\delta y$ and $(k-1)\delta t \leq h \leq k\delta t$.

At any time h , suppose N TTGs stay in $[\vec{x}(h), \vec{y}(h)]$, where $\vec{x}(h) = [x_1(h), x_2(h), \dots, x_N(h)]$ and $\vec{y}(h) = [y_1(h), y_2(h), \dots, y_N(h)]$ indicate the coordinates of each TTG. In order to break the problem in a recursive manner, we introduce two important definitions based on $[\vec{x}(h), \vec{y}(h), h]$.

- $F(\vec{x}, \vec{y}, h)$: the traffic density covered by N TTGs located at positions $[\vec{x}, \vec{y}]$ and time slot h ,

$$F(\vec{x}, \vec{y}, h) = \sum_{k=1}^{n_x} \sum_{l=1}^{n_y} I(k, l, h) f(k, l, h). \quad (9)$$

Given $f(k, l, h)$, $F(\vec{x}, \vec{y}, h)$ is available by the summarization for any $[\vec{x}, \vec{y}, h]$.

- $V(\vec{x}, \vec{y}, h)$: the maximum traffic TTGs can cover from h to n_t , if they start moving from $[\vec{x}, \vec{y}]$. Obviously the boundary condition is

$$V(\vec{x}, \vec{y}, n_t) = F(\vec{x}, \vec{y}, n_t). \quad (10)$$

$V(\vec{x}, \vec{y}, 1)$ is the maximum traffic covered by TTGs if they start at point $[\vec{x}, \vec{y}]$ from the beginning. For all possible starting position $[\vec{x}, \vec{y}]$, $\max_{[\vec{x}, \vec{y}]} (V(\vec{x}, \vec{y}, 1))$ is the maximum traffic covered by all TTGs, which is the solution to the objective function, i.e.,

$$\max_{[\vec{x}(1), \vec{y}(1)]} (V(\vec{x}, \vec{y}, 1)) = \Omega. \quad (11)$$

The dynamic programming based solution starts searching the optimal locations $V(\vec{x}, \vec{y}, h)$ of TTGs from time slot n_t to time slot 1 with the boundary condition $V(\vec{x}, \vec{y}, n_t)$. For each step h , we have obtained $V(\vec{x}, \vec{y}, h+1)$ for any $[\vec{x}, \vec{y}]$ from the previous step, and derive the $V(\vec{x}, \vec{y}, h)$ according to the following analysis.

A. Analysis for the Recursive Method

Suppose $d\vec{x}(h) = [dx_1(h), dx_2(h), \dots, dx_N(h)]$, and $d\vec{y}(h) = [dy_1(h), dy_2(h), \dots, dy_N(h)]$ are the feasible movements of N TTGs at time h . Since $\delta x = \delta y = S * \delta t$, $dx_i(h) = 1, -1$ or 0 and $dy_i(h) = 1, -1$ or 0 in the discrete model. According to the definition, $V(\vec{x}, \vec{y}, h)$ should be the maximum value of the sum of $F(\vec{x}, \vec{y}, h)$ and $V(\vec{x} + d\vec{x}, \vec{y} + d\vec{y}, h+1)$, for all feasible $d\vec{x}, d\vec{y}$. Therefore,

$$\begin{aligned} & V(\vec{x}, \vec{y}, h) \\ &= \max_{d\vec{x}, d\vec{y}} \left\{ V(\vec{x} + d\vec{x}, \vec{y} + d\vec{y}, h+1) + F(\vec{x}, \vec{y}, h) \right\} \\ &= \max_{d\vec{x}, d\vec{y}} \left\{ F(\vec{x}, \vec{y}, h) \delta t + V(\vec{x}, \vec{y}, h) + \frac{\partial V}{\partial h} \right. \\ & \quad \left. + \sum_{i=1}^N \left(\frac{\partial V}{\partial x_i} dx_i + \frac{\partial V}{\partial y_i} dy_i \right) + o(1) \right\}. \end{aligned} \quad (12)$$

where $o(1)$ is the higher-order infinitesimal of the discrete increment 1 of h . Since \vec{x} and \vec{y} are vectors, the derivatives of $V(\vec{x}, \vec{y}, h)$ over \vec{x} and \vec{y} are $\sum_{i=1}^N \left(\frac{\partial V}{\partial x_i} dx_i + \frac{\partial V}{\partial y_i} dy_i \right)$.

When $\delta t \rightarrow 0$ in theory or δt is small enough in the practical system, we can find the derivative of V over h as

$$\begin{aligned} \frac{\partial V(\vec{x}, \vec{y}, h)}{\partial h} &= -\max_{d\vec{x}, d\vec{y}} \left\{ F(\vec{x}, \vec{y}, h) \right. \\ &\quad \left. + \sum_{i=1}^N \left(\frac{\partial V}{\partial x_i} dx_i + \frac{\partial V}{\partial y_i} dy_i \right) \right\} \\ &= -F(\vec{x}, \vec{y}, h) \\ &\quad - \max_{d\vec{x}, d\vec{y}} \sum_{i=1}^N \left(\frac{\partial V}{\partial x_i} dx_i + \frac{\partial V}{\partial y_i} dy_i \right). \end{aligned} \quad (13)$$

With the calculation of $\frac{\partial V}{\partial h}$ in Eq. (13), and the boundary condition in Eq. (10), one can obtain $V(\vec{x}, \vec{y}, 1)$ by

$$V(\vec{x}, \vec{y}, 1) = \sum_{h=1}^{n_t-1} -\frac{\partial V(\vec{x}, \vec{y}, h)}{\partial h} + V(\vec{x}, \vec{y}, n_t). \quad (14)$$

However, the value of $\frac{\partial V}{\partial h}$ depends on another optimization problem, $\max_{d\vec{x}, d\vec{y}} \sum_{i=1}^N \left(\frac{\partial V}{\partial x_i} dx_i + \frac{\partial V}{\partial y_i} dy_i \right)$. Its solution $[d\vec{x}^*, d\vec{y}^*] = \operatorname{argmax}_{d\vec{x}, d\vec{y}} \sum_{i=1}^N \left(\frac{\partial V}{\partial x_i} dx_i + \frac{\partial V}{\partial y_i} dy_i \right)$ guarantees TTGs move to the optimal positions from $h+1$ to h .

Since the definition of $F(\vec{x}, \vec{y}, h)$ already contains the constraint of Eq. (2) by the index variable $I(k, l, h)$, this optimization problem $\max_{d\vec{x}, d\vec{y}} \sum_{i=1}^N \left(\frac{\partial V}{\partial x_i} dx_i + \frac{\partial V}{\partial y_i} dy_i \right)$ has one constraint of Eq. (1). In the discrete model, the speed constraint of Eq. (1) becomes

$$|dx_i| + |dy_i| \leq 1. \quad (15)$$

The constraint of Eq. (15) is for each individual TTG. Two TTGs do not have speed correlation to each other. Therefore,

$$\begin{aligned} \frac{\partial V}{\partial h} &= -F(\vec{x}, \vec{y}, h) \\ &= -\sum_{i=1}^N \max_{dx_i, dy_i} \left(\frac{\partial V}{\partial x_i} dx_i + \frac{\partial V}{\partial y_i} dy_i \right). \end{aligned} \quad (16)$$

So we focus on this smaller optimization problem $\max_{dx_i, dy_i} \left(\frac{\partial V}{\partial x_i} dx_i + \frac{\partial V}{\partial y_i} dy_i \right)$.

The key of this smaller linear optimization problem is to find $\frac{\partial V}{\partial x_i}$ and $\frac{\partial V}{\partial y_i}$, which can be derived numerically. Suppose we have known $V(\vec{x}, \vec{y}, h+1)$ for any $[\vec{x}, \vec{y}]$. Then according to the definition, the left and right derivatives of $\frac{\partial V}{\partial x_i}$ are

$$\begin{aligned} \lrcorner \frac{\partial V}{\partial x_i} &= \frac{1}{\delta x} \left(V([\dots, x_i, \dots], \vec{y}, h+1) \right. \\ &\quad \left. - V([\dots, x_i - \delta x, \dots], \vec{y}, h+1) \right), \end{aligned} \quad (17)$$

$$\begin{aligned} \frac{\partial V}{\partial x_i} \lrcorner &= \frac{1}{\delta x} \left(V([\dots, x_i + \delta x, \dots], \vec{y}, h+1) \right. \\ &\quad \left. - V([\dots, x_i, \dots], \vec{y}, h+1) \right). \end{aligned} \quad (18)$$

Since the left and right derivatives are not necessarily equal, the value of dx_i^* depends on four cases according to the values of $\lrcorner \frac{\partial V}{\partial x_i}$ and $\frac{\partial V}{\partial x_i} \lrcorner$.

- If $\lrcorner \frac{\partial V}{\partial x_i} \geq 0$, $\frac{\partial V}{\partial x_i} \lrcorner \leq 0$, $V(\vec{x}, \vec{y}, h+1)$ reaches the maxima at current point in direction x . Therefore,

$$(dx_i^*, \frac{\partial V}{\partial x_i}) = (0, 0) \quad \text{if} \quad \lrcorner \frac{\partial V}{\partial x_i} \geq 0, \frac{\partial V}{\partial x_i} \lrcorner \leq 0. \quad (19)$$

- If $\lrcorner \frac{\partial V}{\partial x_i} \geq 0$, $\frac{\partial V}{\partial x_i} \lrcorner > 0$, $V(\vec{x}, \vec{y}, h+1)$ increases in direction x . Therefore,

$$(dx_i^*, \frac{\partial V}{\partial x_i}) = (1, \frac{\partial V}{\partial x_i} \lrcorner) \quad \text{if} \quad \lrcorner \frac{\partial V}{\partial x_i} \geq 0, \frac{\partial V}{\partial x_i} \lrcorner > 0. \quad (20)$$

- If $\lrcorner \frac{\partial V}{\partial x_i} < 0$, $\frac{\partial V}{\partial x_i} \lrcorner \leq 0$, $V(\vec{x}, \vec{y}, h+1)$ decreases in direction x . Therefore,

$$(dx_i^*, \frac{\partial V}{\partial x_i}) = (-1, \lrcorner \frac{\partial V}{\partial x_i}) \quad \text{if} \quad \lrcorner \frac{\partial V}{\partial x_i} < 0, \frac{\partial V}{\partial x_i} \lrcorner \leq 0. \quad (21)$$

- If $\lrcorner \frac{\partial V}{\partial x_i} < 0$, $\frac{\partial V}{\partial x_i} \lrcorner > 0$, $V(\vec{x}, \vec{y}, h+1)$ reaches the minimum at point $[x, y]$. Therefore,

$$(dx_i^*, \frac{\partial V}{\partial x_i}) = \begin{cases} (-1, \lrcorner \frac{\partial V}{\partial x_i}) & \text{if} \quad \lrcorner \frac{\partial V}{\partial x_i} < 0, \frac{\partial V}{\partial x_i} \lrcorner > 0 \\ & \text{and} \quad |\lrcorner \frac{\partial V}{\partial x_i}| \geq |\frac{\partial V}{\partial x_i} \lrcorner| \\ (1, \frac{\partial V}{\partial x_i} \lrcorner) & \text{if} \quad \lrcorner \frac{\partial V}{\partial x_i} < 0, \frac{\partial V}{\partial x_i} \lrcorner > 0 \\ & \text{and} \quad |\lrcorner \frac{\partial V}{\partial x_i}| < |\frac{\partial V}{\partial x_i} \lrcorner| \end{cases}. \quad (22)$$

When the left and right derivatives are equal, the solution is simpler, and the equal case has been covered by two cases above, Eq. (20) and Eq. (21).

The solution for dy_i^* is similar to dx_i^* in Eq. (19) to Eq. (22). However, if $|dx_i^*| = |dy_i^*| = \delta x$ from the solution above, the solution breaks the constraint of Eq. (15). Therefore, it is necessary to choose the larger one to optimize $\max_{dx_i, dy_i} \left(\frac{\partial V}{\partial x_i} dx_i + \frac{\partial V}{\partial y_i} dy_i \right)$,

$$(dx_i^*, dy_i^*) = \begin{cases} (dx_i^*, 0) & \text{if} \quad |\frac{\partial V}{\partial x_i}| \geq |\frac{\partial V}{\partial y_i}| \\ (0, dy_i^*) & \text{if} \quad |\frac{\partial V}{\partial x_i}| < |\frac{\partial V}{\partial y_i}| \end{cases}. \quad (23)$$

B. Algorithm

Based on the above analysis, we provide Algorithm 1 to find the optimal TTG trajectories in a recursive manner.

In Algorithm 1, line 1 provides the initial conditions. The loop from line 2 to line 8 is the recursive calculation of $\forall [\vec{x}, \vec{y}], V(\vec{x}, \vec{y}, 1)$. Inside the recursive process, when calculating $V(\vec{x}, \vec{y}, h)$ in any iteration, the previous iteration has provided $\forall [\vec{x}, \vec{y}], V(\vec{x}, \vec{y}, h+1)$, so that line 5 and 6 obtain $[\frac{\partial V}{\partial x_i}, \frac{\partial V}{\partial y_i}]$ and $[dx_i^*, dy_i^*]$ according to Eq. (17) to (23). Line 7 derives $\frac{\partial V}{\partial h}$ according to Eq. (16). With $V(\vec{x}, \vec{y}, h+1)$ and $\frac{\partial V}{\partial h}$, line 8 calculates $V(\vec{x}, \vec{y}, h)$ from the definition of the derivative. $P(x, y, t)$ on line 9 stores the optimal movement of time h , or the position of time $(h+1)$, if the current position is $[\vec{x}, \vec{y}]$. Obviously, the initial value of $P(\vec{x}, \vec{y}, n_t)$ on line 1 is trivial since the TTG will not move anymore at time n_t . After obtaining $\forall [\vec{x}, \vec{y}], V(\vec{x}, \vec{y}, 1)$, line 10 and 11 derive Ω and the corresponding optimal starting point $[\vec{x}^*(1), \vec{y}^*(1)]$ according to Eq. (11). From $[\vec{x}^*(1), \vec{y}^*(1)]$, we can search $P(\vec{x}, \vec{y}, h)$,

Algorithm 1: Search Optimal Trajectories of N TTGs.

input : $\forall [\vec{x}, \vec{y}, h], F(\vec{x}, \vec{y}, h)$
output: Ω , Optimal trajectories $\forall h, [\vec{x}^*(t), \vec{y}^*(t)]$
1 Initial $\Omega = 0$, and
 $\forall [\vec{x}, \vec{y}], V(\vec{x}, \vec{y}, n_t) = F(\vec{x}, \vec{y}, n_t), P(\vec{x}, \vec{y}, n_t) = [\vec{x}, \vec{y}]$;
2 **for** $h \leftarrow (n_t - 1)$ **to** 1 **do**
3 **foreach** $\forall [\vec{x}, \vec{y}], 0 \leq x_i \leq n_x, 0 \leq y_i \leq n_y$ **do**
4 **foreach** $i \leftarrow 1$ **to** N **do**
5 Compute numerical derivative $[\frac{\partial V}{\partial x_i}, \frac{\partial V}{\partial y_i}]$;
6 $[dx_i^*, dy_i^*] = \arg \max \left\{ \frac{\partial V}{\partial x_i} dx_i^* + \frac{\partial V}{\partial y_i} dy_i^* \right\}$;
7 $\frac{\partial V}{\partial h} = -F(\vec{x}, \vec{y}, h) - \sum_{i=1}^N \left\{ \frac{\partial V}{\partial x_i} dx_i^* + \frac{\partial V}{\partial y_i} dy_i^* \right\}$;
8 $V(\vec{x}, \vec{y}, h) = V(\vec{x}, \vec{y}, h + 1) - \frac{\partial V}{\partial h}$;
9 $P(\vec{x}, \vec{y}, h) = [\vec{x} + dx_i^*, \vec{y} + dy_i^*]$;
10 $\Omega = \max_{[\vec{x}, \vec{y}]} \{V(\vec{x}, \vec{y}, 1)\}$;
11 $[\vec{x}^*(1), \vec{y}^*(1)] = \operatorname{argmax}_{[\vec{x}, \vec{y}]} \{V(\vec{x}, \vec{y}, 1)\}$;
12 **for** $h \leftarrow 2$ **to** n_t **do**
13 $[\vec{x}^*(h), \vec{y}^*(h)] = P(\vec{x}^*(h-1), \vec{y}^*(h-1), h-1)$;
14 **return** Ω , and $[\vec{x}^*(t), \vec{y}^*(t)]$

which stores the optimal movement, to obtain the optimal path on line 12 and 13.

The model and the algorithms determine the optimal trajectories of TTGs. However, in real networks, it is impossible and unnecessary to implement all base stations as TTGs. When there is a combination of fixed base stations and TTGs, the model needs minor modifications to account for two cases. The first case is when we supplement TTGs to an existing wireless networks. The fixed base stations in the network have been constructed already, and cannot be re-located to new positions. For those pre-located fixed base stations, the constraint of Eq. (1) is replaced by $x_i(t) = x_i$ and $y_i(t) = y_i$, where $[x_i, y_i]$ is the geometry coordinate of a pre-located fixed base station. The second case is when we design a new network. Although the fixed base stations cannot move, we can choose the optimal positions for them. In this case, the constraint of Eq. (1) for the fixed base stations becomes

$$x_i(t)^2 + y_i(t)^2 \leq 0. \quad (24)$$

With these modifications, the fixed base stations can also be considered as TTGs, and either have fixed positions or have speed as 0.

C. Extension for Limited TTG Capacity

The previous analysis is based on an assumption that the TTG has unlimited capacity. So, in Eq. (9), as long as a point $[k, l, h]$ is in the coverage of any TTG, this TTG is able to forward the traffic from this point to the destination with acceptable delay and packet loss rate. However, TTGs are not always capable of forwarding all traffic generated within their coverage, and multiple TTGs need to cooperate to serve customers in a highly congested area.

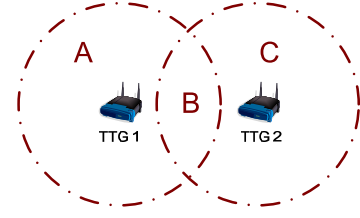


Fig. 3. Limited TTG Capacity vs. Routing

The cooperation among multiple TTGs to forward traffic is inevitably related to the routing strategy for the load balancing. For example, the coverage of two TTGs is shown in Figure 3. Areas A and C are separately covered by TTGs 1 and 2, and area B is covered by both. Suppose the capacity of a TTG is M , and the traffic requirements from areas A, B and C are $r_A = M/4$, $r_B = M/2$, and $r_C = M$. Ideally, if TTG 1 serves the traffic from areas A and B, and TTG 2 serves the traffic from C, the network is able to meet all the demand. However, if the traffic from area B is routed to TTG 2, part of the traffic from area C exceeds the capacity of TTG 2 and suffers performance degradation. Therefore, in order to achieve the optimal results, we have to choose the optimal routing strategy to achieve load balancing.

With the consideration of load balancing, we modify the definitions in Eq. (9) for TTGs with limited capacity. The discrete model provides the feasibility for the numerical analysis for TTGs with limited capacities. Based on the discrete format, we introduce $a^i(k, l, h)$ which indicates the fraction of the traffic from point $[k, l]$ is forwarded by TTG i at time interval h ,

$$0 \leq a^i(k, l, h) \leq 1. \quad (25)$$

With the optimal routing strategy for the load balancing, $F(\vec{x}, \vec{y}, h)$ should be the maximum traffic covered by N TTGs, if their positions are $[\vec{x}, \vec{y}]$ at time interval h . Therefore,

$$F(\vec{x}, \vec{y}, h) = \max_{a^i(k, l, h)} \sum_{k=1}^{n_x} \sum_{l=1}^{n_y} \sum_{i=1}^N a^i(k, l, h) f(k, l, h) \quad (26)$$

such that:

$$\sum_{i=1}^N a^i(k, l, h) \leq 1 \quad (27)$$

$$\sum_{k=1}^{n_x} \sum_{l=1}^{n_y} a^i(k, l, h) * f(k, l, h) \leq M^i \quad (28)$$

$$\text{if } J^i(k, l, h) = 0, \quad a^i(k, l, h) = 0, \quad (29)$$

where $a^i(k, l, h)$ is the decision variable, and M^i is the capacity of TTG k . The constraint of Eq. (27) limits the total fraction of forwarded traffic not to exceed 1; the constraint of Eq. (28) shows that the traffic served by a TTG cannot exceed its capacity; and the constraint of Eq. (29) indicates that the traffic can be forwarded by a TTG, if this point is in its coverage, where $J^i(k, l, h)$ is the index function defined in Eq. (5).

With known $J^i(k, l, h)$ and M^i , the optimization problem of Eq. (26) with constraints of Eq. (27) to (29) can be easily transferred as a linear optimization problem, which can be solved with some efficient algorithms and tools [7, 8].

The proposed algorithms have high complexity. By adjusting the discrete unit, δt , it covers all granularities of the solution, and finds the good balance between the computation complexity and system performance. Additionally, this complex computation is not required in real time, but required when a network is newly constructed or updated. The TTG trajectories depend on the movement of the traffic density $f(k, l, h)$, which seldom vary significantly within a short time. Normally, we expect the optimal TTG trajectories need to be updated every few months. Therefore, the high complexity of the algorithm is not an obstacle.

IV. SIMULATION ANALYSIS

In this section, we compare the performance of the TTG system with the traditional system under different scenarios. Through the performance comparison of the first two scenarios, we show the improvement by TTGs, and analyze some factors influencing the performance. In the third scenario, we apply TTGs to a practical environment, and discuss the feasibility and the economical way to deploy TTGs in real networks.

A. Simulation Setup

The simulation testbed is implemented in Qualnet [9]. In the first two scenarios, the size of the simulation area is 5000×5000 square meters. In the third scenario, the simulation area is as shown in the map of Figure 10. In the simulation, we focus on the WiFi traffic demand, so TTGs are equipped with the WiFi interfaces as the access interface, and 3G interfaces (High-Speed Downlink Packet Access) as the backbone interface. The WiFi access points have the transmission range limits, while the 3G network has ubiquitous coverage in the simulation area. These two interfaces utilize the default protocols at physical and link layers. In the network layer, we use *AODV* [14], which routes packets within the heterogeneous network. In order to simplify the analysis in the simulation, all of the traffic at the application layer is the *constant bit rate* (CBR) over UDP. Since UDP is different from TCP and there is no congestion control and retransmissions, CBR applications enables us to clearly compare the system performance in terms of throughput, delay and packet loss rate. In all figures, the x-axis is the CBR rate of one traffic generators, and the minimum CBR rate on the x-axis is not zero to obtain the valid values of packet loss rate and delay. In each simulation scenario, different numbers of traffic generators and base stations may exist for comparison purpose.

B. Scenario 1: Supplementing an Existing Network with TTGs

This scenario simulates the urban WiFi network in [1] that consists of three areas “Transit”, “Commercial”, and “Residential” parts in the city. In each area, we have two fixed base stations. One TTG moves along the optimal trajectory derived

from Algorithm 1. The traffic generators can be classified as fixed and mobile. There are three fixed traffic generators, each of which stays inside one area, and three mobile traffic generators that move among three areas. In those figures, we compare the system performance with fixed base stations only (*NO-TTG*), and the system with both fixed base stations and TTGs (*TTG*).

Figure 4 shows significant improvement of the system throughput. The major contributions of TTGs come from two aspects. First, in the NO-TTG system, during the movement from one part to another, the customer devices have weak or no connections to the fixed base stations. In the TTG system, TTGs move with the change of the traffic density, and provide much better connections, which improve the throughput. Second, when a large amount of traffic moves into one area, TTGs help fixed base stations to relieve the traffic congestions. The additional resource improves throughput, packet loss rate, and delay.

Figure 5 shows that the packet loss rate of the TTG system is much lower than that of the NO-TTG system. Two reasons result in the packet loss in the system, the transmission failure due to the poor wireless link quality and the buffer overflow due to the high CBR rates. Without TTGs, the weak connections during the movement from one area to another results in the packet loss rate around 15%. In comparison, TTGs provide much better coverage, and keep the packet loss rate at 0%, while the packet loss rate of the NO-TTG system reaches up to 40%. When the CBR rate is high, a large number of packets in NO-TTG system are dropped due to the buffer overflow, since CBR keeps transmitting packets without considering any other flows or congestion control. The packet loss rate is much lower in the TTG system, since it allocates more resources in the congested areas.

Figure 6 shows the average end-to-end packet delay at the application layer. Due to the better coverage and congestion relief, the packet waiting time in the buffer is much less in the TTG system. One unexpected observation is that the delay of the NO-TTG system increases very slowly after a critical CBR rate. The reason is that the calculation of average end-to-end delay is based on the packets successfully received. Higher and higher CBR rates result in higher loss rate, i.e., packets are never delivered. Therefore, the average delay does not increase significantly. In order to understand the performance comparison in a wide range, we enable the CBR rate to increase to a very high level, which may not happen in the real scenarios.

During the simulation, we found that the load balancing is essential to the system performance. First, as the discussion in Section III-C, we need to appropriately choose the routing strategy for load balancing, which enable TTGs to achieve high throughput. Second, other metrics, such as delay and packet loss rate, require good load balancing solution. For example, in Figure 3, if $r_A = r_B = M/4$ and $r_C = M/2$, TTG 2 can serve r_B and r_C while TTG 1 serves r_A . But this strategy leads to higher delay and packet loss rate of traffic from areas *B* and *C*. The optimal solution is that TTG 1 serves

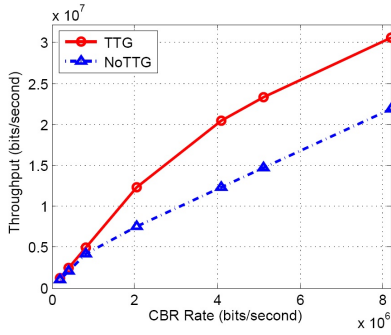


Fig. 4. Throughput of TTG vs. NO-TTG.

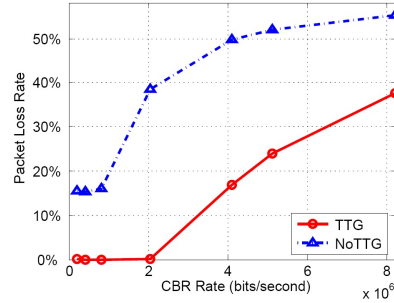


Fig. 5. Packet loss rate of TTG vs. NO-TTG

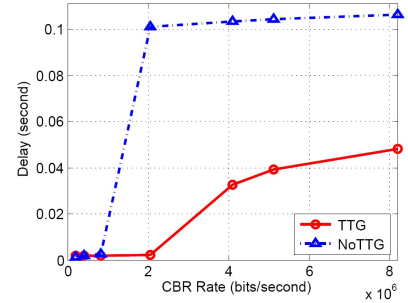


Fig. 6. Delay of TTG vs. NO-TTG.

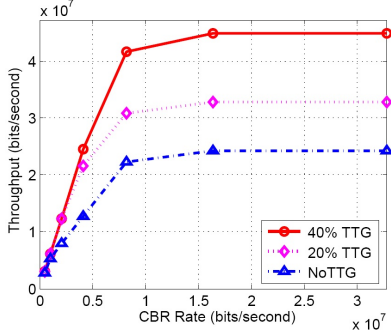


Fig. 7. Throughput as a function of TTG percentage.

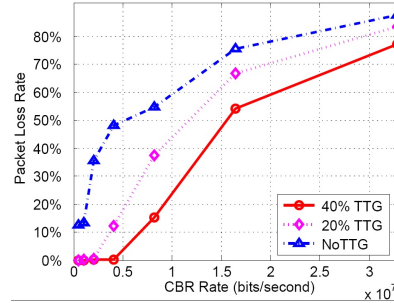


Fig. 8. Packet loss rate as a function of TTG percentage.

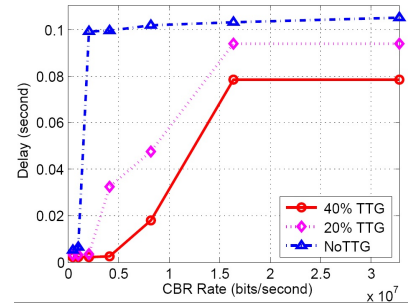


Fig. 9. Delay as a function of TTG percentage.

r_A and r_B , and TTG 2 serves r_C . Significant amount of work has studied load balancing among multiple overlapping base stations. Therefore, the TTG system can employ the exiting algorithms and solutions [10, 11].

C. Scenario 2: Different Percentage of TTGs

The above comparison shows the significant performance improvement, but the TTGs are additional resources. In this section, the scenario is similar to Section IV-B, but we keep 10 base stations including both fixed base stations and TTGs, and gradually substitute the fixed base stations with TTGs. We compare the performance as a function of the percentage of TTGs in the system.

Figure 7 shows the throughput comparison based on different percentage of TTGs. First, more TTGs (40%) enable the system to allocate base stations closer to the traffic sources, which makes the wireless link capacity much higher than that in the system with less (20%) or no TTGs. In addition, more TTGs provide more consistent service according to the distribution of the traffic density at any time. So the system throughput improvement is better with the higher percentage of TTGs.

Figure 8 and Figure 9 show the packet loss rate and average end-to-end delay. The system with higher percentage of TTGs undoubtedly has lower packet loss and delay. Similar to the case in Figure 6, when the throughput is far from the system capacity, the packet loss rate is low and the delay increases according to the CBR rate. However, when the throughput is close to the maximum system capacity, the packet loss rate is high, and the delay flattens. Comparing the CBR rates at

which various systems reach their limits, we find that the upper bound of the system performance with more TTGs is much higher than that of the system without TTGs.

In the performance comparison of this section, we only choose two percentages, 20% and 40%, since we find that the improvement of the system performance does not linearly increase with the percentage of the TTGs. The ratio significantly depends on the traffic distribution. In this scenario, the system needs some base stations to statically stay in a area to serve the fixed traffic. When the percentage of TTGs increases further, part of the optimal TTG trajectories are exactly inside an area with very low mobility. Therefore, the performance improvement does not obviously change even with higher percentage. For example, the upper bound of the system throughput, with 100% of TTGs, is only 10% higher than that of 40% of TTGs. In general, the number of TTGs in a system is an important design parameter. There exists a balance between network performance and operational complexity.

D. Designing TTG Deployment for City of Davis

In the real systems, it may be too costly to allocate TTGs on dedicated vehicles. It is more economical to utilize the public transportation vehicles to carry TTG devices. However, those buses or shuttles cannot exactly follow the optimal trajectories obtained by the algorithms. Fortunately, as long as the bus/shuttle trajectories are approximately close to the optimal trajectories, the system performance is still good. For example, with 100~200 meters of the transmission radius of TTGs' access interface, the system performance is similar if a

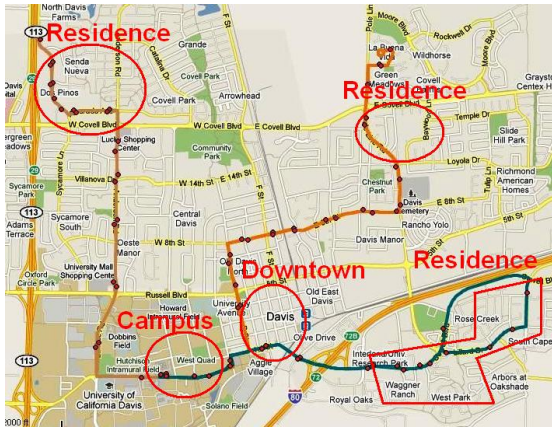


Fig. 10. Selected Bus Routes in City of Davis, CA.

TTG moves along one street or another that is a block away. In order to assess the feasibility of deploying TTGs in the real system, and compare the performance of those sub-optimal trajectories with the optimal ones, we consider a practical TTG deployment scenario in the city of Davis, CA.

We obtain the distribution of access points in Davis from *wigle* [12]. Rather than considering the whole city, we focus on five areas, which have much higher density of access points, as shown in Figure 10. Three of them are residential areas, one is downtown and one is campus. In order to cover the traffic moving between these three residential areas and downtown/campus, three TTGs follow the optimal trajectories to provide better coverage and congestion relief. To compare with those TTGs, we select three bus routes from 14 routes of UNITRANS in Davis, route *J*, route *L* and *W* [13], as shown in Figure 10.

Figure 11 to Figure 13 shows the throughput, packet loss rate and delay of multiple cases. *NO-TTG* stands for the traditional system without TTGs; *Optimal* stands for the system with three TTGs following the optimal trajectories; and *1Bus* stands for the system that has one bus each route that serves as a TTG. Due to the sub-optimal trajectories, the performance of *1Bus* is lower than *Optimal*. In order to reach the comparable performance, we have one more case, *3Bus*, which still has 3 bus routes but each route has 3 buses working as TTGs (The Bus system in Davis provides public transportation service to the entire city with 49 buses on 14 routes).

Figures 11 shows the throughput comparison among different cases. Compared with *NO-TTG*, all of the other three cases have shown the great improvement. The difference between *Optimal* and *1Bus* shows the benefits of the optimal trajectories over the sub-optimal. Those bus routes are closed curves on the map, and buses move along those loops with much shorter periods, such as one or two hours, compared with the period of the traffic density change, such as one day. Therefore, buses cannot always stay in the areas with higher traffic density, and cannot provide the best results. The result of *3bus* is comparative or even better than the *Optimal*, since one or more buses in a route always appear in the congested areas. When one bus moves out of the congested area, another one moves

in and substitutes its place. In addition, since more TTGs serve traffic in both congested and non-congested areas, the result of *3Bus* is better. However, the cost of *3Bus* is much higher, 9 TTGs totally, than that of *Optimal*, 3 TTGs in total.

Figure 12 shows the improvement of the packet loss rate of those TTG systems, *1Bus*, *3Bus* and *Optimal*. Similar to the result of the throughput, the packet loss rates of *Optimal* and *3Bus* are close. But the packet loss rates of *1Bus* and *NO-TTG* are around 6% and 8% even when the CBR rate is low. The reason is the same as discussed in Figure 5 that *1Bus* and *NO-TTG* cannot provide the full coverage, and some packets are dropped, especially when the customers move from “Residence” to “Downtown” or campus.

Figure 13 shows the end-to-end delay improvement among different cases. Two reasons reduce the average delay of the TTG system: (1) the capacity of the wireless links between TTGs and customer devices is usually higher than that between fixed base stations and customer devices, due to shorter transmission distance; and (2) during the congestion, TTGs can shunt traffic resulting in the shorter waiting time in the buffer. One unexpected scenario is that the delay of *3Bus* is much higher than that of *Optimal* at one CBR rate, which is even far from the system capacity. The major reason is the slow handoff between base stations. When one bus enters into an area to substitute the one that is leaving, the routing protocol AODV keeps the traffic to be forwarded to the leaving bus, as long as the link quality is acceptable. Therefore, the poor connections to the leaving TTG increase the average packet delay. Meanwhile, the TTG of the *Optimal* case stays in the congested area, which continuously provides the better wireless connections. But due to the low CBR rate, the traffic can almost be successfully forwarded, so the throughput and packet loss rate of *3Bus* and *Optimal* are comparable. When the CBR rate is high, the probe packets of AODV are easily dropped due to the congestion and weak connections to the leaving TTG, and thus the customer devices scan and quickly switch to the incoming TTG. Since two TTGs of the *3Bus* case serve the traffic, compared with one TTG of the *Optimal* case, the delay of *3Bus* is lower than that of *Optimal*.

V. RELATED WORK

Optimizing the base station locations is an efficient approach to improve the system performance. Liu et al. [15] studied scaling behavior of the throughput capacity with the number of gateways and nodes. S. Sen and B. Raman [16] gave the good problem formulation and solution that incorporates many inter-dependent network variables, such as network topology, antenna types, and performance constraints. With respect to algorithms for gateway placement, there are three main objectives, improving throughput, supporting QoS, and load balancing. To improve the throughput, Li et al. [17] formulated a throughput optimization considering the number of gateways and interference model. Robinson et al. [18] studied how to optimally add new gateways to an existing mesh network. Chen et al. [19] proposed an algorithm to efficiently design the network topology considering the node failure and

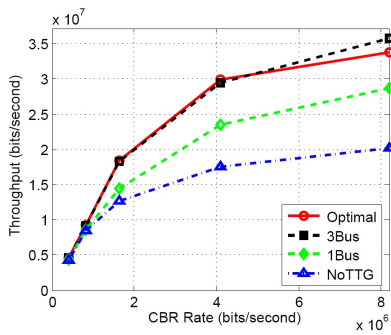


Fig. 11. Throughput in Davis.

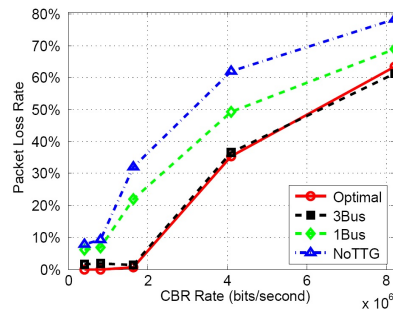


Fig. 12. Packet Loss rate in Davis.

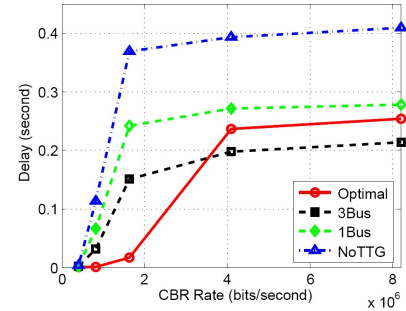


Fig. 13. Delay in Davis.

deployment cost. To support QoS, Aoun et al. [20] proposed a polynomial time near-optimal algorithm to place a minimum number of gateways to satisfy QoS requirement. Benyamina et al. [21] mainly optimized the end-to-end bounded delay communications by a clustering algorithm. For load balancing, Wu et al. [22] modeled the gateway placement as a linear program, and proposed two-stage load balancing, weight-based gateway selection and mesh node attachment. Zeng, and Chen [23] partitioned the network into load-balance and disjointed clusters to balance load among gateways.

However, none of the above studies consider the characteristics of the spatial and temporal changes in the traffic density and use that to optimally locate the base stations. Therefore, it is difficult to achieve both goals of network planning at the same time. In addition, most of the studies, which propose the practical solutions rather than theoretical analysis, focus on the interference mitigation by the integrate solution of routing and scheduling (Chen et al. [19] first discussed the topology formation and then combined it with interference mitigation). The solution based on routing and scheduling is highly dependent on specific platforms. For example, the optimal solution based on WiFi network may not apply to the cellular network. The idea of temporarily adding more base stations/gateways in a football stadium during a game looks similar, but actually different from the TTG system. The gateway in that case is stationary, and serve only one area in a period. It cannot automatically trace traffic density change over time. The proposed algorithm in this paper takes the traffic distribution as the main input instead of the routing or scheduling. Therefore, the algorithm is compatible for multiple platforms, and the optimization result enables TTGs to serve congested traffic in the best locations all the time.

VI. CONCLUSION

In this paper, we propose a novel network component, TTG, to serve as the mobile base station to trace the traffic movement. The TTG system can efficiently locate base stations to the areas with weak wireless connection or congestion, to provide better coverage and relieve congestions. Different from other means to locate the base stations according to specific routing or scheduling algorithms, we propose the model and algorithms to find out the optimal TTG trajectories according to the traffic density distribution during a time period, by a

dynamic programming based solution. Various metrics in the performance verification show the significant improvement of the TTG system in multiple scenarios.

REFERENCES

- [1] M. Afanasyev, T. Chen, G. Voelker, and A. Snoeren, *Analysis of a Mixed-Use Urban WiFi Network: When Metropolitan becomes Neapolitan*, IMC 2008.
- [2] V. Brik, S. Rayanchu, S. Saha, S. Sen, V. Shrivastava, S. Banerjee, *A Measurement Study of a Commercial-grade Urban WiFi Mesh*, IMC 2008.
- [3] C. Song, Z. Qu, N. Blumm, and A. Barabsi, *Limits of Predictability in Human Mobility*, SCIENCE, 2010.
- [4] J. Pang, B. Greenstein, M. Kaminsky, D. McCoy, and S. Seshan, *Wifi-Reports: Improving Wireless Network Selection with Collaboration*, MobiSys 2009.
- [5] D. Kotz and K. Essien, *Analysis of a campus-wide wireless network*, MobiCom, 2002.
- [6] D. Lelescu, U. Kozat, R. Jain, and M. Balakrishnan, *Model T++: An Empirical Joint Space-Time Registration Model*, MOBIHOC, 2006.
- [7] CPLEX: <http://www-01.ibm.com/software/integration/optimization/cplex-optimizer/>
- [8] Premium Solver Platform: <http://solver.com/index.html>
- [9] <http://www.qualnet.com/>
<http://www.scalable-networks.com/products/qualnet/>
- [10] W. Kuo, and W. Liao, *Utility-based radio resource allocation for QoS traffic in wireless networks*, IEEE Transactions on Wireless Communications, 2008.
- [11] C. Luo, H. Ji, and Y. Li, *Utility-Based Multi-Service Bandwidth Allocation in the 4G Heterogeneous Wireless Access Networks*, WCNC, 2009.
- [12] <http://www.wigle.net/>
- [13] <http://www.unitrans.ucdavis.edu/>
- [14] C. Perkins and E. Royer, *Ad hoc On-Demand Distance Vector Routing*, in Proc. of the 2nd IEEE Workshop on Mobile Computing Systems and Applications, 1999.
- [15] B. Liu, Z. Liu, and D. Towsley, *On the capacity of hybrid wireless networks*, INFOCOM 2003.
- [16] S. Sen and B. Raman, *Long distance wireless mesh network planning: problem formulation and solution*, in Proceedings of the 16th international conference on World Wide Web, 2007.
- [17] F. Li, Y. Wang and X. Li, *Gateway Placement for Throughput Optimization in Wireless Mesh Networks*, ICC, 2007
- [18] J. Robinson, M. Uysal, R. Swaminathan, E. Knightly, *Adding capacity points to a wireless mesh network using local search*, INFOCOM, 2008.
- [19] C. Chen, C. Chekuri, and D. Klabjan, *Topology Formation for Wireless Mesh Network Planning*, INFOCOM, 2009.
- [20] B. Aoun, R. Boutaba, Y. Iraqi and G. Kenward, *Gateway Placement Optimization in Wireless Mesh Networks With QoS Constraints*, in Proceeding of JSAC, Nov. 2006.
- [21] D. Benyamina, A. Hafid, and H. Gendreau, *Optimal placement of gateways in multi-hop Wireless Mesh Networks: A clustering-based approach*, LCN, 2009.
- [22] W. Wu, J. Luo, and M. Yang, *Gateway placement optimization for load balancing in wireless mesh networks*, CSCWD, 2009.
- [23] F. Zeng, and Z. Chen, *Load Balancing Placement of Gateways in Wireless Mesh Networks with QoS Constraints*, Young Computer Scientists, 2008.